

## Using the ARGO-YBJ Experiment to Determine the Attenuation and the Absorption lengths

NING CHENG<sup>1</sup> AND MIN ZHA<sup>1</sup> ON BEHALF OF THE ARGO-YBJ COLLABORATION

<sup>1</sup>*Institute of High Energy Physics, BeiJing 100049, P.R.China*  
 chengning@ihep.ac.cn

**Abstract:** Using the data taken by the ARGO-YBJ experiment (606 g/cm<sup>2</sup>, Tibet, P.R.China) since July to December 2006, with the measurement of the EAS size spectrum, the attenuation length is calculated on the method of constant intensity cut, and the absorption length is also determined. By comparing with the result from the ARGO-YBJ test experiment, our preliminary results show a good consistency.

### 1. Introduction

The decrease of shower size ( $N_e$ ) with increasing atmospheric depth ( $X$ ) after the shower size maximum in Extensive Air Shower (EAS) is usually described by the attenuation length ( $\lambda_{att}$ ):

$$\langle N_e(X) \rangle \propto e^{-\frac{X}{\lambda_{att}}} \quad (1)$$

While the decrease of integral flux for showers with  $N_e$  greater than a constant value is described by the absorption length ( $\lambda_{abs}$ ):

$$J(> N_e, X) \propto e^{-\frac{X}{\lambda_{abs}}} \quad (2)$$

Some researches have been performed by KASCADE (1046 g/cm<sup>2</sup>) [1], EAS TOP (810 g/cm<sup>2</sup>) [2], MAKET ANI (700 g/cm<sup>2</sup>) [3], etc. In this analysis the preliminary results obtained with the data from ARGO-YBJ 130 Clusters are presented.

### 2. The Detector Set-up

The ARGO-YBJ experiment, located at YangBa-Jing, Tibet, P.R.China (latitude 30.1° N, longitude 90.5° E, 4300 m a.s.l., 606 g/cm<sup>2</sup>), is a collaboration between Chinese and Italian institutes. The apparatus consists of a full coverage array of dimension 78 x 74 m<sup>2</sup> made of a single layer of Resistive Plate Chambers (RPCs), 125 x 280 cm<sup>2</sup> each. The area surrounding the central carpet, up

to 110 x 100 m<sup>2</sup>, which is called the guard ring, is partially (20%) instrumented with RPCs. The whole array (154 Clusters of RPCs) has been installed and the full central carpet (10 x 13 Clusters) has been put into operation since June 2006. More details of detector can be found in [4] and the RPC performance has been extensively described in [5]. A real strip-pattern of an event is shown in **Figure 1**, the minimum unit of this graph being the Pad, so at most 8 Strips can be hit (see the palette).

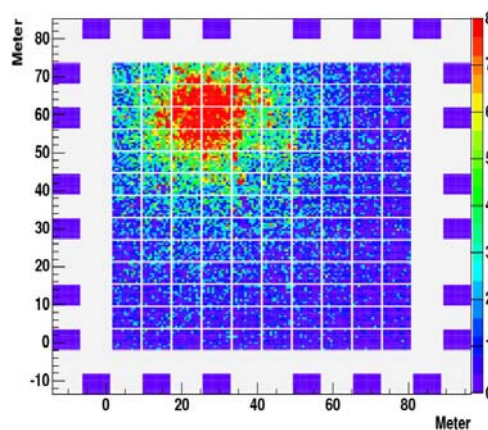


Figure 1: An EAS event detected by ARGO-YBJ. The palette on the right is the number of fired Strips on a Pad.

A full Monte Carlo simulation has been used to understand the detector performance and to check the selection criteria used in this analysis. On the base of CORSIKA 6500 [6], with the GHEISHA and QGSJET II interaction models, a large number of showers initiated by primary protons have been generated in the energy region from 10 TeV to 10 PeV, with the spectrum index of -2.7 and the incident angle isotropically sampled within  $0-45^\circ$ . The full detector response has been simulated by ARGOG, a tool based on GEANT3 [7] package and developed by the ARGO-YBJ collaboration. A full array with  $10 \times 13$  Clusters, 95% detector trigger efficiency,  $110 \times 100 \text{ m}^2$  sampling areas (the sampling area is bigger enough considering the cut to select the internal showers, to be described later) and Low Multiplicity 20 (which means the number of fired pads  $\geq 20$ ) are used in the Monte Carlo simulation. The simulated proton samples are then reconstructed in an iterative procedure: After the first guess for the direction by fitting the arrival times and positions of triggered pads in a plane fit, with the standard NKG function, the lateral distribution of the fired strips and a fixed conical parameter  $\alpha=0.03$  for shower front plane, the shower core ( $X_c$ ,  $Y_c$ ) and size ( $N_e$ ) can be estimated on the base of the maximum likelihood method. The above reconstruction procedure can be iterated several times in order to reject some noisy pads with too low or too high signals and achieve a better  $\chi^2$  value.

In order to select internal showers and improve the reconstruction quality, we first set three pre-selections: (1) the fired pad multiplicities of the shower is higher than 5000 ( $N_{\text{pad}} > 5000$  is corresponding to  $\sim 50$  TeV for proton initiated shower in the vertical direction); (2) the zenith angle is less than  $40^\circ$ , (3) the reconstructed shower core is inside the central  $6 \times 9$  clusters. The simulation shows that the angular resolution is much better than  $1^\circ$ , while for the shower initiated by protons with energy of 100 TeV, the resolution of shower core position is better than 1 m and the shower size resolution,  $\delta N_e / N_e$ , is around 10%.

### 3. Data Analysis

Data taken in the operation period of July to December 2006 are used for the analysis. After using the same reconstruction procedure and applying the selection criteria described above, a total of more than 2 million events remains with  $N_{\text{pad}} > 5000$ . **Figure 2** shows the comparison of the zenith angle distribution obtained from data and simulation samples, thus demonstrating a good agreement. The correlation between the simulated shower size and the reconstructed size is shown in **Figure 3**: a good linearity with slope parameter close to 1 testifies the reliability of the reconstruction method.

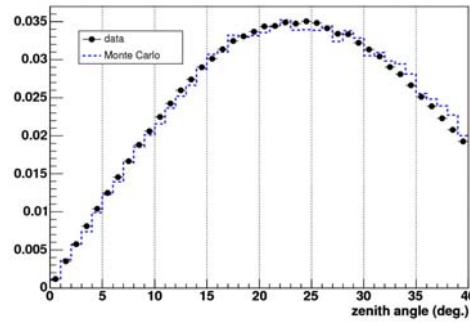


Figure 2: The distribution of Zenith angles. Error bars for the data are smaller than the point sizes.

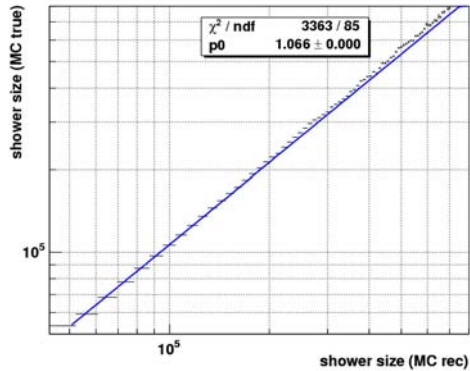


Figure 3: The correlation between the simulated shower size and reconstructed size.

#### 3.1 Attenuation Length $\lambda_{\text{att}}$

As a next step of our analysis, in order to avoid the contamination from the low energy events and

the mis-reconstructed high energy ( $\sim$  PeV) events due to saturation effects, we just consider the shower with size within the region of  $4 \times 10^4$ - $5 \times 10^5$ . The method of Constant Intensity Cut (CIC) is used to infer the attenuation length. The shifts of the shower sizes ( $N_e$ ) are analyzed at eight different integral intensity values in the range from  $10^{-5.3}$  to  $10^{-6} \text{ m}^{-2}\text{s}^{-1}\text{sr}^{-1}$ , as shown in **Figure 4**. The distribution of them is expected to follow an exponential behavior in **Eq. 3**.

$$I(\theta) = I(0)e^{-\frac{X_0}{\lambda_{att}}(\sec\theta-1)} \quad (3)$$

Where  $I(\theta)$  and  $I(0)$  are the integral intensity of the shower size with zenith angle at  $\theta$  and the vertical direction respectively;  $X_0$  is the vertical observation depth. The attenuation lengths versus different integral intensities are plotted in **Figure 5**. The attenuation length increases from 175 to 200 g/cm<sup>2</sup> with the decrease of selected intensity, i.e., from right to left direction in the abscissa, which implies that the primary energy goes higher as well. Our measurement is more close to the shower maximum position as long as the energy increases, so a more flat longitudinal profile of the shower is expected. Due to different observation altitudes, we can not directly compare our attenuation lengths with KASCADE results; however the similar tendency with the increase of intensity is obvious.

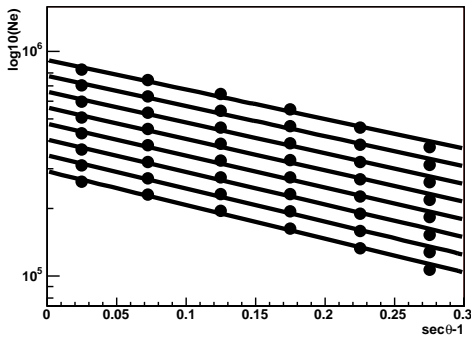


Figure 4: Shower size  $N_e$ , as a function of zenith angle for different fixed intensity values. From the top to the bottom line, the intensity cut values are  $10^{-6}$ ,  $10^{-5.9}$ ,  $10^{-5.8}$ ,  $10^{-5.7}$ ,  $10^{-5.6}$ ,  $10^{-5.5}$ ,  $10^{-5.4}$ ,  $10^{-5.3} \text{ m}^{-2}\text{s}^{-1}\text{sr}^{-1}$ , respectively.

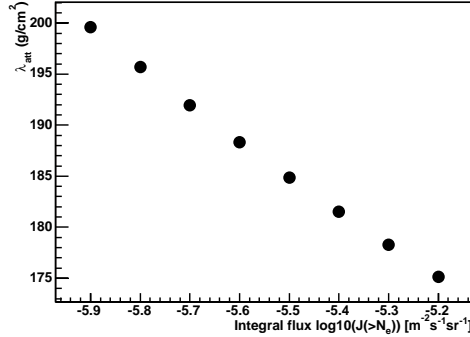


Figure 5: Attenuation lengths versus different intensity values.

### 3.2 Absorption Length $\lambda_{abs}$

Conforming to the definition in **Eq. 2**, an exponential fit to the decrease of integral flux for the different  $N_e$  thresholds yields the absorption length. The detailed information is shown in **Figure 6** and **Figure 7**. Just as the attenuation length, the absorption length shows the same tendency with the increasing primary energy.

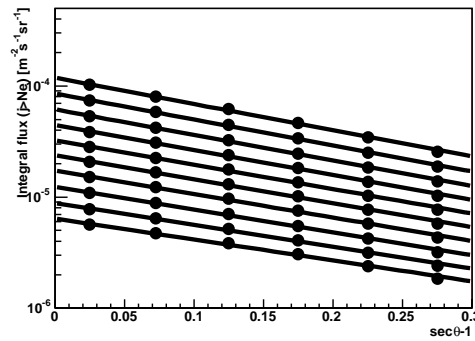


Figure 6: Integral intensity as a function of zenith angle for different constant  $N_e$ . From the top to the bottom line, the fixed shower size  $N_e$  are  $10^{4.55}$ ,  $10^{4.65}$ ,  $10^{4.75}$ ,  $10^{4.85}$ ,  $10^{4.95}$ ,  $10^{5.05}$ ,  $10^{5.15}$ ,  $10^{5.25}$ ,  $10^{5.35}$ ,  $10^{5.45}$ , respectively.

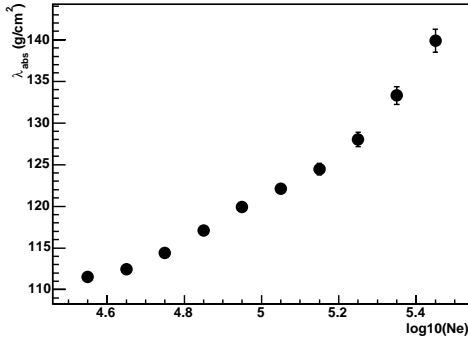


Figure 7: Absorption lengths versus  $N_e$ .

As shown in Figure 7, the value of this measurement is basically consistent with the previous results [4, 8]. In those studies, by measuring the angular distribution of events with particle density exceeding a certain value, the absorption of air showers in the atmosphere has been discussed. As discussed in details in [3], with the assumption of pure composition and a simple power law of the shower size distribution, a simple relation exists between the absorption length and the attenuation length,  $\lambda_{att} = \gamma \lambda_{abs}$ , where  $\gamma$  is the integral size spectra index. In average our measurements show the index value is around 1.5.

#### 4. Conclusion and Discussions

Using the ARGO-YBJ data taken in the period of July to December 2006, the digital read-out of the strip is analyzed. With a preliminary measurement of the shower size spectrum, the attenuation length and the absorption length are calculated. Both values show a good consistency with the previous results [4, 8].

As presented in [9], a first result about p-air cross section measurement around several TeV is discussed by using the ARGO-130 clusters data. However, the absorption length calculated in this analysis is different from the one used to infer the p-air cross section. In this analysis for a constant shower size, a certain range of primary energies are involved, thus the absorption length combines not only the different first interaction point,  $X_0$ , but also the contribution of the shower attenuation. So in principle it is not directly correlated with p-air cross section by a simple function.

Despite the shower fluctuation plays a major role in the measurement of p-air cross section with the typical EAS method [10], with the merit of the high altitude of the ARGO-YBJ experiment, which means less shower fluctuations in the observation, our future plan is to find an independent way of fixing the primary energy and constraining the shower attenuation, and to explore the p-air cross section in the higher energy region.

#### References

- [1] T. Antoni et al. (KASCADE Coll.), *Astroparticle Phys.* 19 (2003) 703.
- [2] M. Aglietta et al., *Astroparticle Phys.* 10 (1999) 310
- [3] A.A. Chilingarian, arXiv: astro-ph/0002076, 2000.
- [4] C. Bacci et al. (ARGO-YBJ Coll.), *Astroparticle Phys.* 17 (2002) 151.
- [5] G. Aielli et al. (ARGO-YBJ Coll.), *NIM A* 562 (2006) 92.
- [6] J. Knapp and D. Heck, *Extensive Air Shower Simulation with CORSIKA* (1998).
- [7] CERN Program Library Group Writeup W5013 (1994).
- [8] P. Bernardini et al., on behalf of the ARGO-YBJ Coll., ICRC 2005 (Pune)
- [9] I. De Mitri et al., on behalf of the ARGO-YBJ Coll., Proton-air inelastic cross section measurement with ARGO-YBJ. In this conference, 2007.
- [10] J. Alvarez-Muniz et al., *Phys. Rev. D* 69 (2004) 103003.